Transition Metal Chemistry (2018) 43:65–72
https://doi.org/10.1007/s11243-017-0194-0

Transition metal complexes of a hydrazone derived from hydralazine hydrochloride and 3,5-di-tert-butylsalicylaldehyde

Sunil M. Patil[1] · Ramesh S. Vadavi[2] · Suneel Dodamani[3] · Umashri Kendur[1] · Geeta Chimmalagi[1] · Sunil Jalalpure[3,4] · Christopher S. Frampton[5] · Kalagouda B. Gudasi[1]

Received: 4 October 2017 / Accepted: 15 November 2017 / Published online: 22 November 2017

Abstract
Mononuclear Co(III), Ni(II) and Cu(II) coordination compounds of (*E*)-1-(3,5-di-tert-butyl-2-hydroxybenzylidene)-2-(phthalazin-1-yl)hydrazine (**LH**) were prepared and characterized by physicochemical and spectroscopic methods. The metal-to-ligand ratio was found to be 1:2 in $[Co(\mathbf{L})_2]Cl{\cdot}2H_2O$ (**1**) and $[Ni(\mathbf{L})_2]{\cdot}2H_2O$ (**2**), while it is 1:1 in $[Cu(\mathbf{L})Cl]{\cdot}2CH_3OH$ (**3**). The X-ray crystal structures of **LH** and complex **1** is are reported. **LH** shows monobasic behavior, coordinating through NNO donor atoms. The complexes were investigated for their antimicrobial properties. Complexes **1** and **3** show excellent antibacterial and antifungal activities, respectively.

Introduction

Microbial drug resistance is an ongoing challenge in medicinal chemistry [1, 2]. Association of an organic drug with a metal atom can enhance the activity of the organic moiety [3, 4]. Furthermore, coordination compounds with varied geometries and charge can show targeted interactions with biomolecules such as DNA, RNA and phospholipids [5]. A wide range of ligands and their transition metal complexes show good activities against bacteria including *S. aureus, E. coli, P. putida* and *B. subtilis* [6–8].

Due to their facile synthesis, structural diversity and good solubility in common solvents, hydrazones are among the most widely used ligands for the synthesis of coordination compounds [9, 10]. The reaction of hydrazones with metal ions can lead to coordination compounds with interesting medicinal properties, as observed in benzimidazoles [11] pyrimidines [12], pyridines [13] and quinazolines [14]. Furthermore, chelation masks the polarity of the metal ion, due to sharing of its positive charge with the donor atoms. This increases the lipophilic nature of the metal, so enhancing the migration of the metal through the lipid layers of the microorganisms [15].

Hydralazine hydrazones (**HH**) are widely synthesised through simple condensation of a carbonyl compound with the hydrazine group. **HH**s show a wide range of applications, in areas from bioscience to materials science [16–20]. The potential coordination sites of **HH** are the phthalazine and azomethine nitrogen atoms. The chelating ability of **HH** can be extended by placing a suitable donor atom at the ortho-position of an aromatic carbonyl compound. Salicylaldehyde derivatives and their metal complexes have shown potent inhibition against a number of microbial species [21, 22]. Furthermore, compounds with tertiary-butyl substituents can show enhanced biological activity [23]. In view of the above points, we have synthesised transition metal complexes of a hydrazone obtained from the condensation of hydralazine hydrochloride with 3,5-di-tert-butylsalicylaldehyde (Scheme 1). The synthesised complexes have been

Electronic supplementary material The online version of this article (https://doi.org/10.1007/s11243-017-0194-0) contains supplementary material, which is available to authorized users.

✉ Kalagouda B. Gudasi
drkbgudasi@kud.ac.in

[1] Department of Chemistry, Karnatak University, Dharwad, Karnataka 580003, India

[2] Y. B. Annigeri Pre-University Science and Commerce College, Dharwad, India

[3] Dr. Prabhakar Kore Basic Science Research Center, KLE Academy of Higher Education and Research, KLE University, Belagavi, Karnataka 590010, India

[4] Department of Pharmacognosy, College of Pharmacy, KLE Academy of Higher Education and Research, KLE University, Belagavi, India

[5] Brunel University London, Uxbridge UB8 3PH, UK

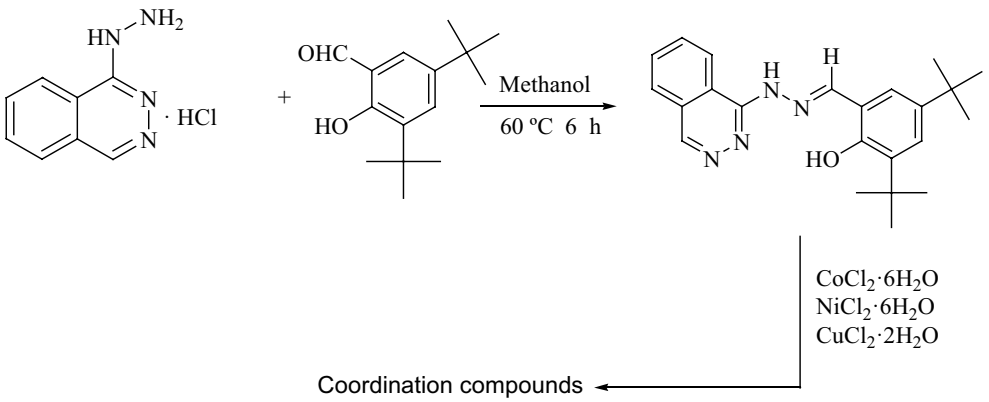

Scheme 1 Synthesis of the **LH** and **1–3**

screened for antimicrobial activity. The results of our studies are reported in this paper.

Experimental

Materials and methods

3,5-Di-tert-butyl-2-hydroxybenzaldehyde and hydralazine hydrochloride were obtained from Sigma-Aldrich and used as received. Cobalt(II) chloride hexahydrate and nickel(II) chloride hexahydrate, copper(II) chloride dihydrate and solvents were purchased from S. D. Fine chemicals. Solvents were of reagent grade and used without additional purification. Elemental analysis was performed on an Elementar Analysensysteme GmbH instrument. IR spectra were recorded in the region of 4000–400 cm^{-1} on a Nicolet 170 SX FTIR spectrometer (KBr disk matrix). ^{1}H and ^{13}C NMR spectra were recorded in DMSO-d_6 on a Bruker FT 400 MHz spectrometer with TMS as internal standard. ESI mass spectral data for the complexes were obtained using a Waters UPLC-TQD mass spectrometer. UV–Vis absorption spectra were recorded on a JASCO UV–Vis NIR spectrophotometer (Model V-670). Thermal studies were carried out with a TGA7 analyzer (PerkinElmer, USA) in the temperature range 25–1000 °C at a heating rate of 10 °C min^{-1} in an oxygen atmosphere.

X-ray diffraction data for **LH** and complex **1** were collected on an Oxford Diffraction (Agilent Technologies), SuperNova X-ray diffractometer equipped with an Oxford Cryosystems Cobra low-temperature device using Cu-K_α radiation (α = 1.54184 and 1.54178 Å) from a fine-focus sealed X-ray tube SuperNova Cu X-ray microsource and focusing mirror optics. The structures were solved by direct methods and refined against F^2 by full-matrix least squares using the program SHELXTL [24]. The H atoms were located in a difference map, but those attached to carbon atoms were repositioned geometrically. The H atoms were initially refined with soft restraints on the bond lengths and angles to regularize their geometry, after which the positions were refined with riding constraints [25]. All non-hydrogen atoms were refined anisotropically. Molecular structures were drawn using ORTEP [26], and all the intermolecular interactions were visualized using Mercury version 3.9 [27].

Preparation of LH

A solution of hydralazine hydrochloride (0.83 g, 4.26 mmol) and 3,5-di-tert-butyl-2-hydroxybenzaldehyde (1 g, 4.26 mmol) in methanol (40 mL) was stirred at 60 °C for 6 h. Solvent from the resultant dark solution was removed under reduced pressure. The pale green residue so obtained was washed with water, filtered off and recrystallized from the minimum amount of methanol.

Yield 1.4 g (89%). Anal. calcd. (%) for $C_{23}H_{28}N_4O$: C, 73.3; H, 7.5; N, 14.8; found: C, 73.1: H, 7.1; N, 14.6. ^{1}H NMR (400 MHz, DMSO-d6) δ: 12.17 (s, 1H) 11.03 (s, 1H), 8.65 (s, 1H), 8.30 (d, J = 7.2 1H), 8.13 (s, 1H), 7.79–7.71 (m, 3H), 7.33–7.27 (m, 2H) 1.43 (s, 9H) 1.27 (s, 9H) ^{13}C NMR (DMSO-d6, δ ppm): 158.6, 154.3, 146.1, 140.2, 138.0, 135.0, 132.2, 131.8, 126.8, 126.5, 126.4, 126.0, 125.1, 123.6, 118.2, 34.5, 33.8, 31.2, 29.3. FTIR bands (KBr, ν/cm^{-1}): 3416.53 (br), 3348 (m), 2950 (m), 1616 (s), 1594 (s), 1537 (m), 1481 (m), 1026 (m) MS: m/z $[M]^+$ 376.

Preparation of the complexes

To a hot solution of **LH** (0.5 g, 1.3 mmol) in methanol (30 mL), a solution of the required metal salt (1.5 mmol $CoCl_2·6H_2O$/$NiCl_2·6H_2O$/$CuCl_2·2H_2O$) in the minimum amount of methanol was added; the mixture was refluxed for 3–6 h. The precipitate obtained was filtered off, washed thoroughly with methanol and dried under vacuum.

$[Co(L)_2]Cl{\cdot}3H_2O$ (1) Yield 0.86 g (71%). Anal. calcd. (%) for $C_{46}H_{60}ClCoN_8O_5$: C, 61.4; H, 6.7; N, 12.4; found: C, 61.4: H, 6.4; N, 12.3. ^{1}H NMR (400 MHz, DMSO-d6) δ: 14.77 (s, 1H), 8.97 (br, s, 1H), 8.72–8.61 (m, 2H), 8.06–7.92 (m, 3H), 7.34 (s, 3H), 7.00 (s, 1H) 1.24 (s, 9H) 0.73 (s, 9H) ^{13}C NMR (DMSO-d6, δ ppm): 160.6, 150.0, 141.2, 140.8, 135.1, 134.6, 133.8, 127.6, 127.4, 127.1, 123.9, 116.6, 108.4, 108.2, 35.2, 33.9, 31.8, 29.4. FTIR bands (KBr, ν/cm^{-1}): 3438 (br), 2954 (s), 1609 (m), 1589 (m), 1572 (w), 1543 (s), 1524 (s), 1460 (w) 1424 (s), 1169 (s). MS: *m/z*; [M] $^+$ 809.39 (calculated 809.37 for $C_{46}H_{54}CoN_8O_2$.

$[Ni(L)_2]{\cdot}2H_2O$ (2) Yield 0.82 g (69%). Anal. calcd. (%) for $C_{46}H_{58}N_8NiO_4$: C, 68.2; H, 6.7; N, 13.8; found: C, 68.1: H, 6.3; N, 13.5. FTIR bands (KBr, ν/cm^{-1}): 3429 (br), 2954 (s), 1599 (br), 1535 (s), 1477 (w), 1531 (w), 1259 (m), 1171 (s). MS: *m/z*; $[M + H]^+$ 809.36 (calculated 809.38 for $C_{46}H_{54}NiN_8O_2$.

$[Cu(L)Cl]{\cdot}CH_3OH$ (3) Yield 0.67 g (75%). Anal. calcd. (%) for $C_{25}H_{35}ClCuN_4O_3$: C, 55.7; H, 6.5; N, 10.4; found: C, 55.6: H, 6.2; N, 10.1. FTIR bands (KBr, ν/cm^{-1}): 3446 (br), 2954 (s), 1610 (m), 1590 (m), 1542 (s), 1422 (m), 1171 (s). MS: *m/z*; $[M–Cl]^+$ 438.16 (calculated 438.15 for $C_{23}H_{27}CuN_4O$).

Antibacterial activity

The susceptibilities of the test organisms to these compounds were assessed using broth dilution assays, as minimum inhibitory concentration (MIC). Assays were performed in triplicate. *S. aureus* Microbial Type Culture Collection (MTCC) 12598, *S. mutans* MTCC 25175, E. *coli* MTCC 443 and *P. aeruginosa* MTCC 25668 were selected for the study. All the bacteria were previously subcultured in brain heart infusion (BHI) media, and its sterility was assessed at 35 °C for 48 h prior to testing of the vehicles.

Broth dilution method

The minimum inhibitory concentration was carried out by serial dilution. A 200 µl aliquot of BHI broth was added to ten microtitre tubes (2 ml). A 200 µl aliquot of the test compound (100 µl/ml) was added to first and second tubes and then was serially diluted from the second tube up to the ninth. The optical density of the bacterial culture (CFU) was adjusted to 0.5 Mcfarland standards, and 50 µl of bacterial suspension was added to each tube, except for the negative control, such that the first and last tubes served as positive and negative control, respectively. The lowest concentration of test compound showing growth inhibition was recorded

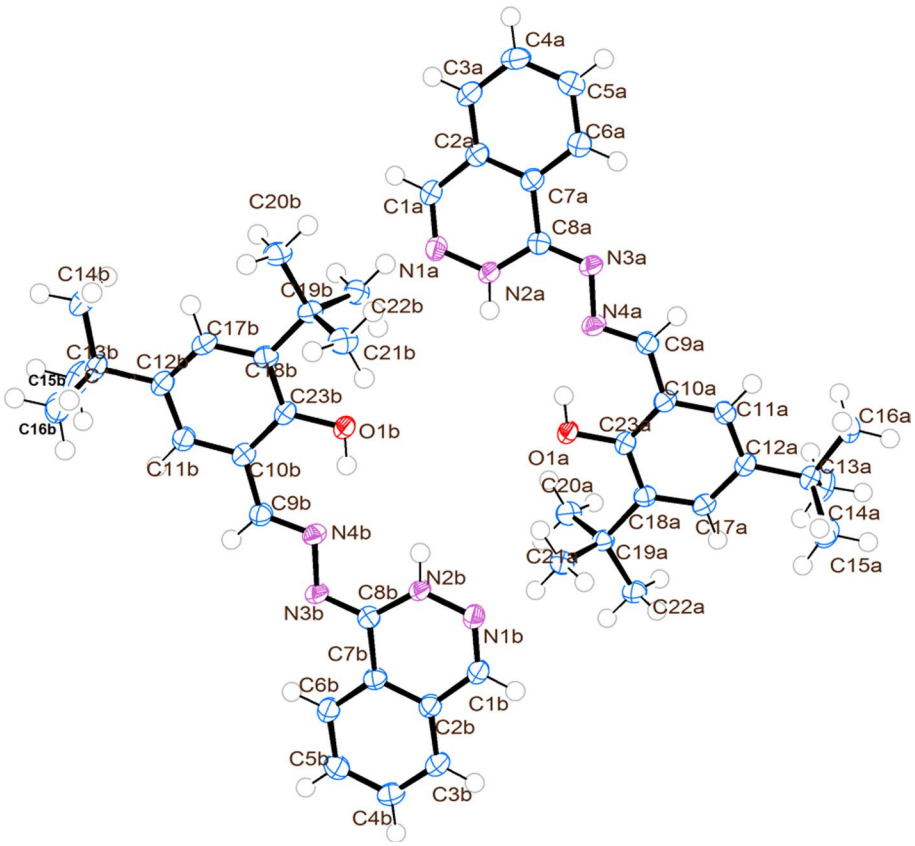

Fig. 1 ORTEP projection of **LH** showing 30% probability ellipsoids

as the MIC. The standard antibiotic ciprofloxacin (10 µg/ml) was used as the reference.

Antifungal activity

The fungi *Aspergillus fumigatus* (MTCC13073), *Aspergillus flavus* (MTCC 2017), *Candida albicans* (MTCC 2011) and *Aspergillus niger* and other microorganisms used were obtained from the Dr. Prabhakar Kore Basic Science Research Centre, KLE University, Belagavi, India. The MIC of each test compound against the isolates was determined using microdilution techniques, in accordance with the CLSI method. A sterile 200 µl sample of BHI media was added to each tube. The first tube acted as positive control and the tenth as negative control. A 200 µl aliquot of test compound with 100 µg/ml concentration was added to the first tube and serially diluted. A 20 µl aliquot (10^4–10^6 cfu) of culture was added to each tube. The standard antifungal fluconazole (10 µg/ml) was used as the reference. The tubes were observed after 48 h for the change in turbidity at 600 nm. The final range of the concentration of the test compounds was between 0.2 and 100 µg/mL.

Results and discussion

The proligand **LH** was synthesized in good yield. Single crystals of **LH** suitable for X-ray diffraction studies were obtained by slow evaporation of a methanolic solution, while crystals of complex **1** were obtained by vapor diffusion technique (diethyl ether/methanol). Efforts to grow crystals of complexes **2** and **3** were unsuccessful. In complex **1,** the Co(II) ion has undergone oxidation to Co(III).

X-ray diffraction and spectroscopic studies

ORTEP diagrams of **LH** and complex **1** are depicted in Figs. 1 and 2 along with atom numbering schemes. The crystal structure refinement data for both compounds are compiled in Table 1, and selected bond lengths and angles are given in Table 2. Free **LH** crystallizes in the monoclinic system in space group P121/n1. There are two molecules in the asymmetric unit which are related only by pseudo-symmetry. A bond distance of 1.293 (1) Å between C(1)–N(1) indicates double-bond nature. The bond lengths for N(1A)–N(2A), C(8A)–N(2A) and C(8A)–N(3A) are 1.370 (1), 1.371 (1)

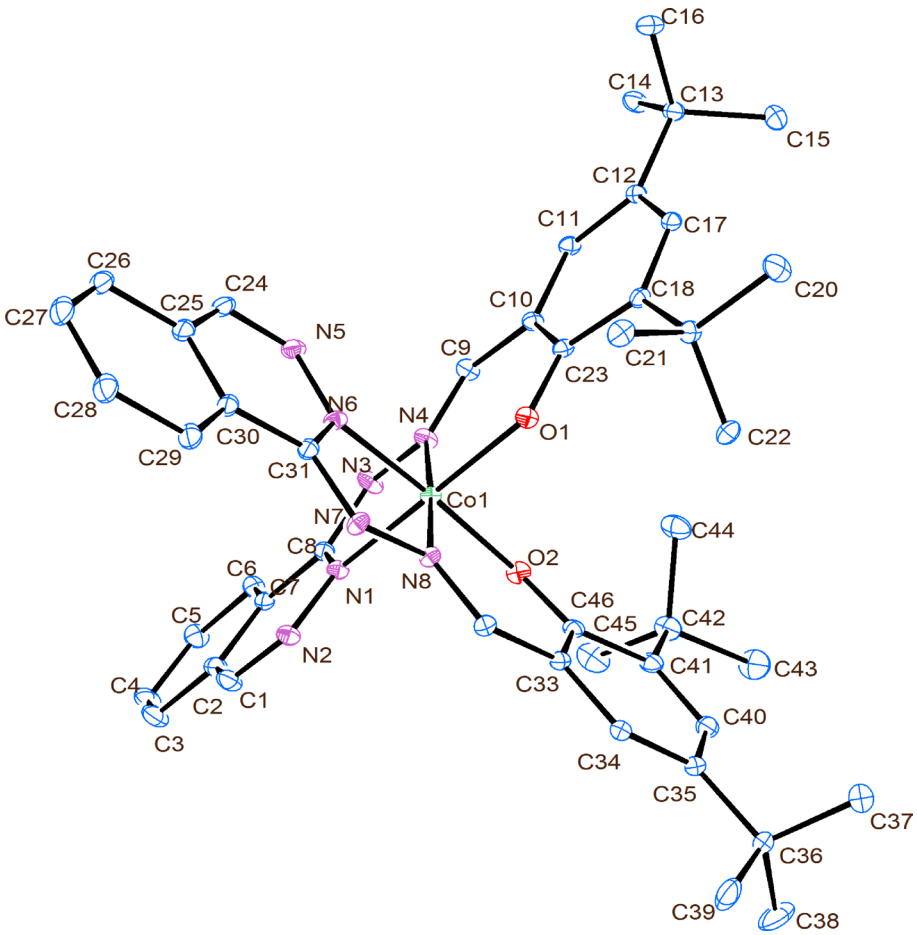

Fig. 2 ORTEP projection of 1 showing 30% probability ellipsoid

Table 1 Crystal data and structure refinement for the **LH** and **1**

Empirical formula	$C_{23}H_{28}N_4O$	$C_{48}H_{59}ClCoN_8O_{2.50}$
Formula weight	376.49	882.41
Temperature	100(2) K	100(2) K
Wavelength	1.54178 Å	1.54178 Å
Crystal system	Monoclinic	Orthorhombic
Space group	*P* 21/*n*	*P b c n*
a/Å	11.88270(10)	*a* = 38.9963(9) Å
b/Å	16.6222(2)	*b* = 11.5934(3) Å
c/Å	20.5141(2)	*c* = 21.0289(5) Å
α/°	90	90
β/°	90.9210(10)	90
γ/°	90	90
Volume	4051.35(7) Å^3	9507.1(4) Å^3
Z	8	8
Density (calculated)	1.235 Mg/m^3	1.233 Mg/m^3
Absorption coefficient	0.609 mm^{-1}	3.714 mm^{-1}
F(000)	1616	3736
Crystal size	0.30 × 0.14 × 0.08 mm^3	0.20 × 0.06 × 0.05 mm^3
Theta range for data collection	3.42°–74.49°	2.27°–74.49°
Range *h*	−14 to 11	−48 to 43
Range *k*	−20 to 20	−14 to 14
Range *l*	−25 to 24	26 to 26
Reflections collected	18,011	26,080
Refinement method	Full-matrix least squares on F^2	Full-matrix least squares on F^2
Data/restraints/parameters	8263/0/533	9710/0/566
Goodness of fit on F^2	1.035	1.009
Final *R* indices [$I > 2$sigma(I)]	$R1 = 0.0353$, $wR2 = 0.0992$	$R1 = 0.0490$, $wR2 = 0.1109$
R indices (all data)	$R1 = 0.0390$, $wR2 = 0.1025$	$R1 = 0.0735$, $wR2 = 0.1224$
CCDC	1,570,625	1,570,623

and 1.300 (1) Å, respectively [16], suggesting a single bond between endocyclic nitrogen atoms N(1A) and N(2A), and C(8A)–N(2A) with a double bond between C(8A)–N(3A). These values support the location of the acidic proton to endocyclic nitrogen N(2A) (Fig. S1). In **LH**, N(2A)–H(2A) is involved in intermolecular hydrogen bonding with N(1A) to form a dimer (Fig. S2). An intramolecular hydrogen bond is found between the phenolic OH and azomethine nitrogen, [O(1A)···H(1C)–N(4A)]. The phenolic oxygen is involved in C-H···O type interactions, O(1A)···C1A-H(1A) and O(1A)···C(21A)-H(21A). The plane of the phthalazine ring makes an angle of 14.9º (2) with that of the phenyl ring (Fig. S3).

Complex **1** crystallizes in the orthorhombic system in space group Pbcn. The structure has dimerized; it is a monochloride salt. One molecule is present in the asymmetric unit. There is an additional well ordered and fully occupied diethyl ether solvate molecule located on a two-fold axis, making the overall structure a hemi-diethyl ether solvate (packing diagram, Fig. S4). The chloride anion is slightly disordered with an occupancy ratio of 92.9:7.1. The disorder appears to be a result of the potential H-bonding interactions.

In complex **1**, **LH** acts as a monobasic ligand, coordinating through the phthalazine N(2A), azomethine N(4A) and phenolic O(1A) atoms to form a CoN_4O_2 octahedral configuration. The average Co–N [1.891(2) Å] and Co–O [1.881(5) Å] bond lengths are in the same ranges as those found in similar octahedral Co(III) systems [28, 29] and considerably shorter than the equivalent bond lengths to Co(II). The bond distance of 1.299 (1) Å between C(1)–N(1) indicates double-bond nature. The bond lengths of 1.366 (1), 1.331 (1) and 1.348 (1) Å for N(1A)–N(2A), C(8A)–N(2A) and C(8A)–N(3A), respectively, suggest a single bond between the endocyclic nitrogen atoms N(1A) and N(2A), with more of a double-bond character for C(8A)–N(2A). This indicates that the imine proton is shifted from endocyclic N2A to exocyclic N3A during complexation. A classical hydrogen bond is observed between the imine proton (H3) and chloride counterion [N3–H3···Cl] (Fig S5). The angle between the

Table 2 Selected bond lengths of **LH** and **1**

Bond lengths [Å]		Bond angles [°]	
Crystallographically independent molecule A of **LH**			
O1A–C23A	1.360(1)	N3A–N4A–C9A	110.65(8)
N4A–N3A	1.397(1)	N4A–N3A–C8A–	114.63(7)
N4A–C9A	1.291(1)	N2A–N1A–C1A–	117.18(8)
N3A–C8A	1.300(1)	N1A–N2A–C8A	126.34(8)
N1A–N2A	1.370(1)	O1A–C23A–C18A	119.98(8)
N1A–C1A	1.293(1)	O1A–C23A–C10A	119.53(8)
N2A–C8A	1.371(1)	C18A–C23A–C10A	120.49(8)
Crystallographically independent molecule B of **LH**			
O1B–C23B	1.360(1)	N3B–N4B–C9B	111.28(8)
N4B–N3B	1.396(1)	N4B–N3B–C8B	114.42(7)
N4B–C9B	1.292(1)	N2B–N1B–C1B	117.10(8)
N3B–C8B	1.302(1)	N1B–N2B–C8B	126.56(8)
N1B–N2B	1.370(1)	O1B–C23B–C18B	119.99(8)
N1B–C1B	1.292(1)	O1B–C23B–C10B	119.45(8)
N2B–C8B	1.371(1)	C(18B)–C(23B)–C(10B)	120.56(8)
Coordination compound **1**			
Co(1)–N(8)	1.869(2)	N(8)–Co(1)–N(4)	177.28(10)
Co(1)–N(4)	1.873(2)	N(8)–Co(1)–O(2)	94.04(8)
Co(1)–O(2)	1.8741(18)	N(4)–Co(1)–O(2)	87.10(9)
Co(1)–O(1)	1.8876(18)	N(8)–Co(1)–O(1)	88.49(9)
Co(1)–N(1)	1.910(2)	N(4)–Co(1)–O(1)	94.00(9)
Co(1)–N(5)	1.913(2)	O(2)–Co(1)–O(1)	89.26(8)
O(1)–C(23)	1.317(3)	N(8)–Co(1)–N(1)	94.59(9)
N(3)–N(4)	1.383(3)	N(4)–Co(1)–N(1)	82.94(9)
N(4)–C(9)	1.288(3)	O(2)–Co(1)–N(1)	89.42(9)
N(3)–C(8)	1.348(3)	O(1)–Co(1)–N(1)	176.72(9)
N(1)–N(2)	1.365(3)	N(8)–Co(1)–N(5)	82.87(9)
N(2)–C(8)	1.331(3)	N(4)–Co(1)–N(5)	95.90(9)
		O(2)–Co(1)–N(5)	176.34(9)
		O(1)–Co(1)–N(5)	92.61(9)
		N(2)–Co(1)–N(5)	88.87(9)
		C(23)–O(1)–Co(1)	126.46(16)
		C(46)–O(2)–Co(1)	125.76(16)

planes of the phthalazine and pyridine rings is decreased to 8.27° (7) on complexation.

The IR spectrum of free **LH** shows bands at 3416 and 3348 cm^{-1}, assignable to ν(OH) and ν(NH), respectively. Participation of the phenolic group in coordination is confirmed by the observed shift in the (C–O) stretching frequency to higher wavenumbers [30]. Deprotonation of the phenolic OH is confirmed by ^{1}H NMR and single-crystal XRD studies. Strong bands at 1616 and 1594 cm^{-1} can be assigned to (C=N) and (C=N ring) groups, respectively, which are shifted to lower energies on coordination of **LH** to the metal.

The ^{1}H NMR spectrum of the **LH** is shown in Fig. S6. The signals at 12.17, 11.03 and 8.65 ppm are assigned to the imine proton [N(2A)H], phenolic proton [O(1A)H] and azomethine proton (C(9A)H), respectively. The signals in the ranges of 7.71–8.65 and 7.27–7.33 ppm are assigned to the aromatic protons of the phthalazine ring and salicylaldehyde, respectively. The tertiary-butyl groups are observed as singlets at 1.27 and 1.43 ppm. The absence of a signal from a phenolic proton in the spectrum of complex **1** confirms deprotonation and hence coordination of phenolic OH (Fig. S7). The downfield shift of the NH proton (14.37 ppm) can be accounted for by transfer of the proton from endocyclic nitrogen N2A to exocyclic nitrogen N3A, which is involved in hydrogen bonding with the chloride ion. In general, all of the protons are deshielded upon complexation of **LH**, indicating sharing of electron density with the metal center.

The carbons C8, C9 and C23, which are observed at 158.6, 146.1 and 154.3 ppm, respectively, in the ^{13}C NMR spectrum of the free proligand, are shifted to 160.6 141.2 and 150.0 ppm in the spectrum of complex **1**, indicating coordination of **LH** through the phthalazine nitrogen, azomethine nitrogen and phenolic oxygen atoms.

Electronic spectra of the complexes are shown in Fig. S8. The Co(III) complex shows a charge transfer band at 457 nm, which may also obscure the d–d transitions [31]. The Ni(II) complex shows a charge transfer band at 460 nm and features at 969 and 732 nm assignable to $^{3}A_{2}g \rightarrow {}^{3}T_{2}g(F)$ and $^{3}A_{2}g \rightarrow {}^{3}T_{1}g(F)$ d–d transitions, respectively. These transitions indicate an octahedral geometry around the Ni(II)

Table 3 Antibacterial activity, measured as minimum inhibitory concentration (MIC), of the ligand and its coordination compounds

Compound	Minimum inhibitory concentration (μg/ml)			
	P. aeruginosa	*S. mutans*	*S. aureus*	*E. coli*
LH	1.56	12.5	25	6.25
1	1.56	3.125	6.25	1.56
2	25	3.125	25	6.25
3	6.25	25	3.125	1.56
Ciprofloxacin	1.56	12.5	3.125	3.125

Table 4 Antifungal activity, measured as minimum inhibitory concentration (MIC), of the ligand and its coordination compounds

Compound	Minimum inhibitory concentration (μg/ml)			
	A. flavus	*A.fumigatus*	*A.niger*	*C. albicans*
LH	50	100	50	50
1	25	50	25	25
2	50	20	50	12.5
3	12.5	12.5	6.25	12.5
Fluconazole	6.25	12.5	6.25	6.25

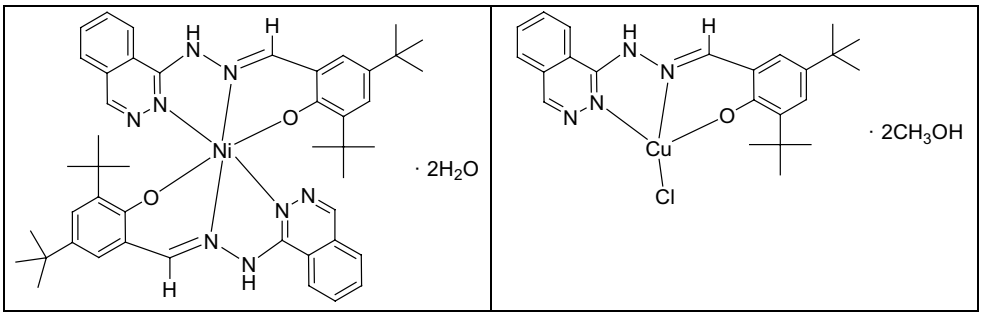

Fig. 3 Tentatively assigned structures for **2** and **3**

atom. The Cu(II) complex shows a medium intensity broadband around 611 nm assigned to the $^2T_2 \rightarrow {}^2E$ transition in a tetrahedral geometry [32].

Thermal studies

Thermograms of the complexes are given in Figs. S16–S18. Their decomposition processes include two steps. In the first, there is loss of solvent/counter anions, followed by decomposition of the ligand in the second step. For complex **1,** an initial weight loss of 5.9% below 90 °C is assigned to the loss of three lattice water molecules (calc. 6.01%). The chloride ion was lost between 255 and 310 °C (expt. 3.90%, calc. 4.08%). This is followed by loss of two ligand molecules, leaving behind the metal oxide. For complex **2**, a weight loss of 4.32% (calc. 4.26%) occurred below 95 °C and corresponds to the loss of two lattice water molecules. The ligand part decomposed above 200 °C (expt. 86.01%, calc. 88.90%). For copper complex **3**, a weight loss below 70 °C is assigned to the loss of two lattice methanol molecules (expt. 11.50%, calc. 11.92%). This is followed by loss of chloride between 210 and 250 °C. Finally, the ligand decomposed above 280 °C and a plateau above 750 °C is attributed to the metal oxide.

Antibacterial and antifungal activities

The antimicrobial activities of the synthesised compounds were evaluated using the broth dilution method in triplicate experiments [33]. The MIC values are reported in µg/ml. The antibacterial activity was tested against gram-positive *S. aureus* and *S. mutans* and gram-negative *E. coli* and *P. aeruginosa*, using ciprofloxacin as a standard. Antifungal activity was tested against *A. flavus*, *A. niger*, *C. albicans* and *A. fumigatus* using fluconazole as reference. The data obtained are summarized in Tables 3 and 4.

Free **LH** showed activity against *P. aeruginosa*; however, against the rest of the species its activity is modest. The cationic Co(III) complex showed excellent inhibition against all the bacterial species and was more effective against gram-negative bacteria, which may be due to more effective electrostatic interactions. Complex **2** showed better inactivation of *S. aureus,* a pathogenic gram-positive bacterium. Complex **3** is highly toxic against *E. coli* compared to the standard ciprofloxacin.

Free **LH** has low activities against the fungal strains used; however, its activity was enhanced upon metal association. Antifungal activities with MIC 50 µg/ml were observed for all of the complexes. In particular, the copper complex (**3**) showed excellent activity comparable to fluconazole [34].

Conclusions

A new ligand (*E*)-1-(3,5-di-tert-butyl-2-hydroxybenzylidene)-2-(phthalazin-1-yl)hydrazine and its complexes $[Co(\mathbf{L})_2]Cl{\cdot}2H_2O$ (**1**), $[Ni(\mathbf{L})_2]{\cdot}H_2O$ (**2**) and $[Cu(\mathbf{L})Cl]{\cdot}2CH_3OH$ (**3**) have been prepared and characterized. **LH** shows monobasic, NNO tridentate behavior in these complexes. Complexes **1** and **2** have 1:2 metal-to-ligand ratio and distorted octahedral geometries, whereas complex **3** has a 1:1 metal-to-ligand ratio and tetrahedral geometry (Fig. 3). The complex **1** shows excellent activity against gram-negative bacteria, while complex **3** shows excellent antifungal activity.

Supplementary data

CCDC 1570625 and 1570623 contain the supplementary crystallographic data for the **LH** and **1**, respectively. These data can be obtained free of charge via http://www.ccdc.cam.ac.uk/conts/retrieving.html or from the Cambridge Crystallographic Data Centre, 12 Union Road, Cambridge CB2 1EZ, UK; fax: (044) 1223-336- 033; or e-mail: deposit@ccdc.cam.ac.uk.

Acknowledgements Authors Sunil M. Patil, Umashri Kendur and Geeta Chimmalagi are thankful to University Grants Commission for providing UGC-UPE fellowship and Research Fellowship in Sciences for Meritorious Students (UGC-RFSMS).Thanks are due to USIC, Karnatak University, Dharwad, for spectral analysis.

References

1. World Health Organization (2001) WHO global strategy for containment of antimicrobial resistance. WHO, Geneva
2. Kalinowska-Lis U, Felczak A, Checinska L, Zawadzka K, Patyna E, Lisowska K, Ochocki J (2015) Dalton Trans 44:8178–8189
3. Karpin GW, Morris DM, Ngo MT, Merola JS, Falkinham JO (2015) Med Chem Commun 6:1471–1478
4. Yu M, Nagalingam G, Ellis S, Martinez E, Sintchenko V, Spain M, Rutledge PJ, Todd MH, Triccas JA (2016) J Med Chem 59:5917–5921
5. Li F, Collins JG, Keene FR (2015) Chem Soc Rev 44:2529–2542
6. Ng NS, Leverett P, Hibbs DE, Yang Q, Bulanadi JC, Wu MJ, Aldrich-Wright JR (2013) Dalton Trans 42:3196–3209
7. Neelakantan MA, Esakkiammal M, Marriappan SS, Dharmaraja J, Jeyakumar T (2010) Indian J Pharm Sci 72:216–222
8. Ming LJ (2003) Med Res Rev 23:697–762
9. Stadler AM, Harrowfield J (2009) Inorg Chim Acta 362:4298–4314
10. Carmona-Vargas CC, Váquiro IY, Jaramillo-Gómez LM, Lehn JM, Chaur MN (2017) Inorg Chim Acta 468:131–139
11. Arjmand F, Mohani B, Ahmad S (2005) Eur J Med Chem 40:1103–1110
12. Easmon J, Pürstinger G, Heinisch G, Roth T, Fiebig HH, Holzer W, Jäger W, Jenny M, Hofmann J (2001) J Med Chem 44:2164–2171
13. Mishra A, Kaushik NK, Verma AK, Gupta R (2008) Eur J Med Chem 43:2189–2196
14. Hoonur RS, Patil BR, Badiger DS, Vadavi RS, Gudasi KB, Dandawate PR, Ghaisas MM, Padhye SB, Nethaji M (2010) Eur J Med Chem 45:2277–2282
15. Ahmed RM, Yousif EI, Hasan HA, Mo J, Al-Jeboori MJ (2013) Sci World J 2013:1–7
16. Nfor EN, Husian A, Majoumo-Mbe F, Njah IN, Offiong OE, Bourne SA (2013) Polyhedron 63:207–213
17. Hollo B, Magyari J, Zivkovic-Radovanovic V, Vuckovic G, Tomic ZD, Szilagyi IM, Pokol G, Szecsenyi KM (2014) Polyhedron 80:142–150
18. El-Sherif AA, Shoukry MM, Abd-Elgawad MMA (2012) Spectrochim Acta A Mol Biomol Spectrosc 98:307–321
19. Patil S, Fegade U, Sahoo SK, Singh A, Marek J, Singh N, Bendre R, Kuwar A (2014) ChemPhysChem 15:2230–2236
20. Lee JJ, Choi YW, You GR, Lee SY, Kim C (2015) Dalton Trans 44:13305–13314
21. Shi L, Ge HM, Tan SH, Li HQ, Song YC, Zhu HL, Tan RX (2007) Eur J Med Chem 42:558–564
22. Aslan HG, Özcan S, Karacan N (2011) Inorg Chem Commun 14:1550–1553
23. Hadida S, Goor FV, Zhou J, Arumugam V, McCartney J, Hazlewood A, Decker C, Negulescu P, Grootenhuis PDJ (2014) J Med Chem 57:9776–9795
24. Sheldrick GM (2001) SHELXTL. Version 5.0. Bruker AXS Inc., Madison
25. Cooper RI, Thompson AL, Watkin DJ (2010) J Appl Cryst 43:1100–1107
26. Burnett MN, Johnson CK (1996) Oak Ridge National Laboratory Report ORNL-6895
27. Macrae CF, Bruno IJ, Chisholm JA, Edgington PR, McCabe P, Pidcock E, Rodriguez-Monge L, Taylor R, van de Streek J, Wood PA (2008) J Appl Crystallogr 41:466–470
28. Ware DC, Wilson WR, Denny WA, Rickard CEF (1991) J Chem Soc Chem Commun 1171–1173. doi:http://doi.org/10.1039/C39910001171
29. Ammar RA, Alaghaz AMA, Zayed ME, Al-Bedair LA (2017) J Mol Struct 1141:368–381
30. Lee JJ, Choi YW, You GR, Lee SY, Kim C (2015) Dalton Trans 44:13305–13314
31. Singh NK, Tripathi P, Bharty MK, Srivastava AK, Singh S, Butcher RJ (2010) Polyhedron 29:1939–1945
32. Karabocek N, Kucukdumlu A, Senses E, Karabocek S, Ozcimder R (2011) Synth React Inorg Met Org Nano-Met Chem 41:1095–1101
33. Chougala BM, Samundeeswari S, Holiyachi M, Shastri LA, Dodamani S, Jalalpure S, Dixit SR, Joshi SD, Sunagar VA (2017) Eur J Med Chem 125:101–116
34. Ng NS, Leverett P, Hibbs DE, Yang Q, Bulanadi JC, Wu MJ, Aldrich-Wright JR (2013) Dalton Trans 42:3196–3209